Chapter 4

Simulation and Measurement

4.1 Simulation

In this section, the spot size is simulated by OSLO software. The simulation case includes two parts, one is for only fiberlens component and the other is for fiberlens component with SIL. Because of each component is fabricated by different process, so it may have different limitation in fabrication process. We aim at each component to simulate each condition which may occur in fabrication process. In order to obtain a reliable simulation data and results, the parameters setting of simulation condition will adopt the actual fabrication results of each component. Finally, the simulation results will compare with the measurement results, and are discussed in the following. All components and variables in simulation condition are shown in Fig.4-1. Here, because of mirror doesn't influence the output beam quality, so we ignore the mirror in simulation condition.

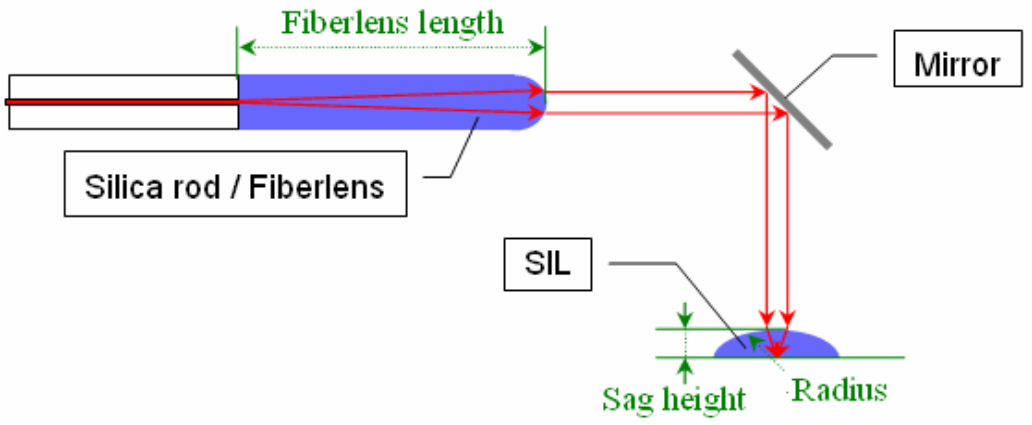

Fig.4-1 All components and variables in simulation condition

4.1.1 Fiberlens

The shape of fiberlens is made by cohesion, and the radius of fiberlens is 62.5 μm which is the minimum radius of fiberlens we can make. In simulation condition setting, the refractive index of fiberlens and air are 1.47 and 1.0, respectively. Figure 4-2 shows the fiberlens simulation setup. The spot size is defined by the minimum beam width, and the N.A. is defined by $sin\theta$. Figure 4-3 shows the simulation results which the fiberlens length versus N.A. and spot size. The N.A. is linear relation with fiberlens length, and the spot size is similar exponent decay.

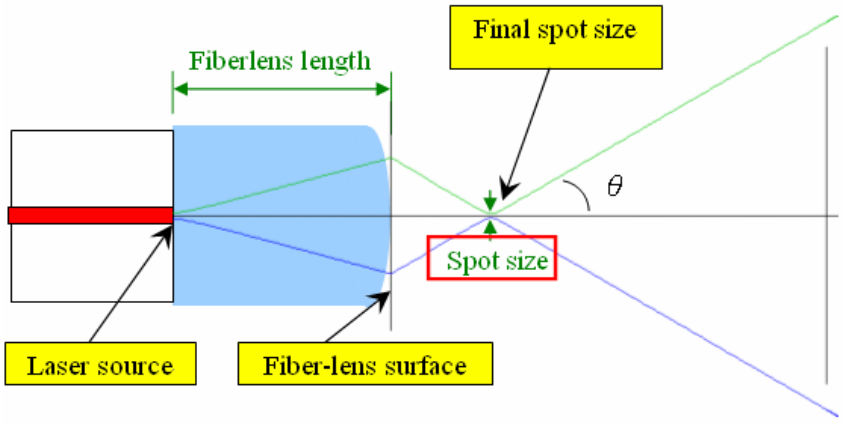

Fig.4-2 The fiberlens simulation setup

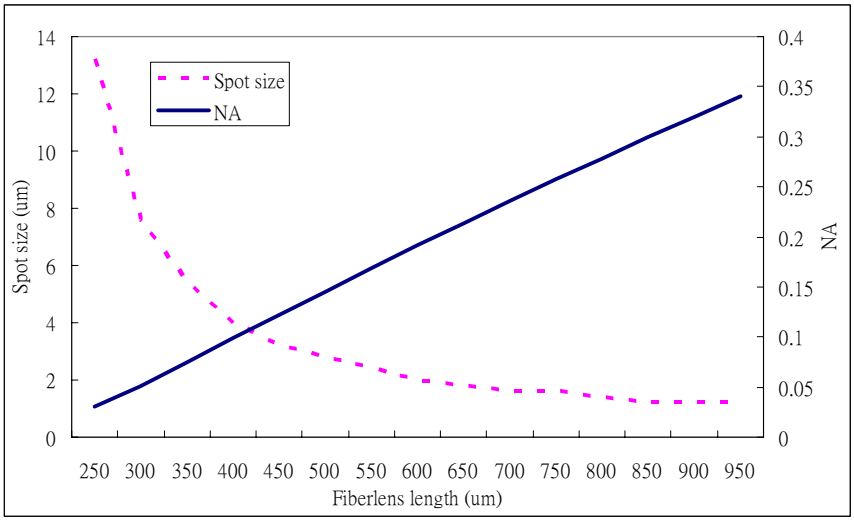

Fig.4-3 Fiberlens length vs. Spot size and NA

As shown in Fig.4-3, when the radius and length of fiberlens are is 62.5 μm and 465 μm, respectively, The N.A. of fiberlens is about 0.14, and the spot size is about 3.0 μm.

4.1.2 Fiberlens and SIL

Here, the fiberlens combines SIL component with two different sizes, and are simulated by OSLO software. The parameters of SIL size are shown in Tab.4-1. We assumed that the surface profile of SIL is a perfect hemisphere. Figure 4-4 shows refractive index of AZ-4620 20μm versus the thermal reflowing time at 150°C, this are measured by ellipse-meter. When SIL is heated at 150°C for 2.5 hours in fabrication process, the refractive index of SIL is about 1.63. The refractive indexes in simulation condition setting are listed in Tab.4-2.

Tab.4-1 The parameters of SIL size

	Diameter (μm)	***Sag height (μm)***	***Radius (μm)***
SIL	φ60	30.00	30.00
	φ70	31.50	35.19

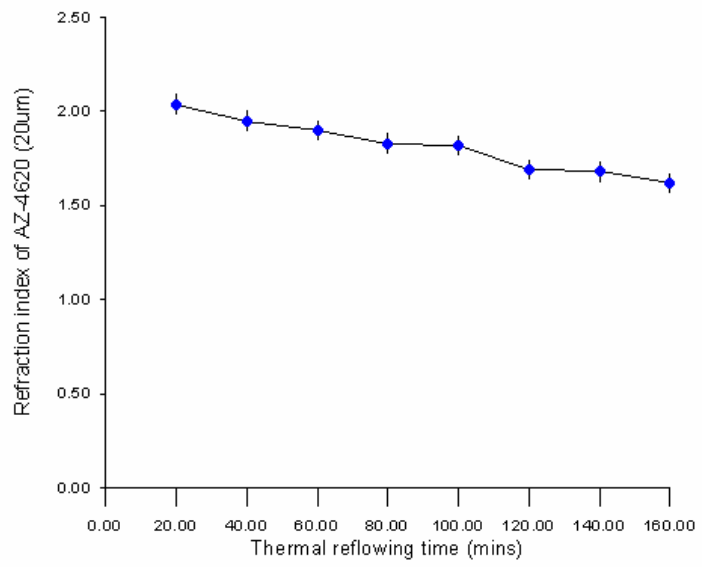

Fig.4-4 Refraction index of AZ-4620 20μm versus thermal reflowing time at 150°C

Tab.4-2 The refractive indexes in simulation condition setting

Interface	*Refractive index*
Fiberlens	1.47
Air	1
45°mirror	1
SIL	1.63

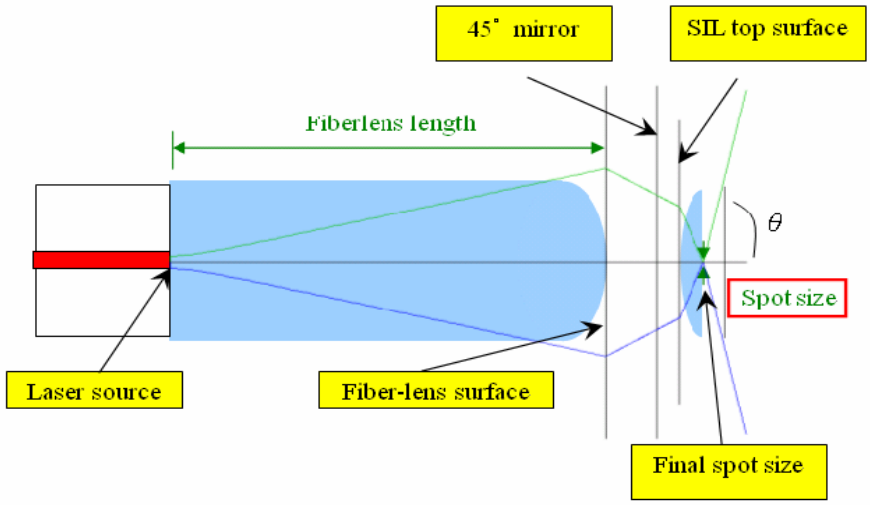

Fig.4-5 The simulation setup of fiberlens combining the SIL component

Tab.4-3 The simulation results of fiberlens combining SIL

	Diameter (μm)	*Spot size (μm)*
Fiberlens	*--*	***3.00***
SIL	φ60	1.88
	φ70	2.03

Figure 4-5 shows the simulation setup of fiberlens combining the SIL component, and the simulation results are listed in Tab.4-3. When a fiberlens spot size of diameter 3.0 μm is put into the SIL component, and then is focused again by SIL. The spot size can shrink further. From this simulation results, we found that the SIL of diameter 60 μm and 70 μm can shrink spot size from 3.0 μm to 1.88 μm and 2.03 μm, respectively. The SIL of diameter 60 μm and 70 μm have 37.4% and 32.4%

shrinkage efficiency, respectively. This simulation results will be compared and discussed with measurement results in the following.

4.2 Measurement

In this research, the self-alignment verification, spot size calibration, and reliability of SIL are measured with the far-field experiment setup which is assembled by us. The measurement results and discussion will be presented in the following.

A co-focal system was used to broaden the output beam and measure the spot size, as shown in Fig.4-6, because the focused spot size of the NFR pick-up head is less than 3μm from previous simulation, comparatively smaller than the pixel size of CCD camera, which is about 5μm to 10μm generally. The incident beam passes through the NFR pick-up head, and is focused between the NFR pick-up head and objective lens. The output beam from objective lens will be collimated, when the focused spot is adjusted to be positioned in the focal plane of the objective lens. Finally, the output beam is detected by CCD camera. The spot size of output beam is defined as full-width at $1/e^2$ maximum intensity, as shown in Fig.4-7.

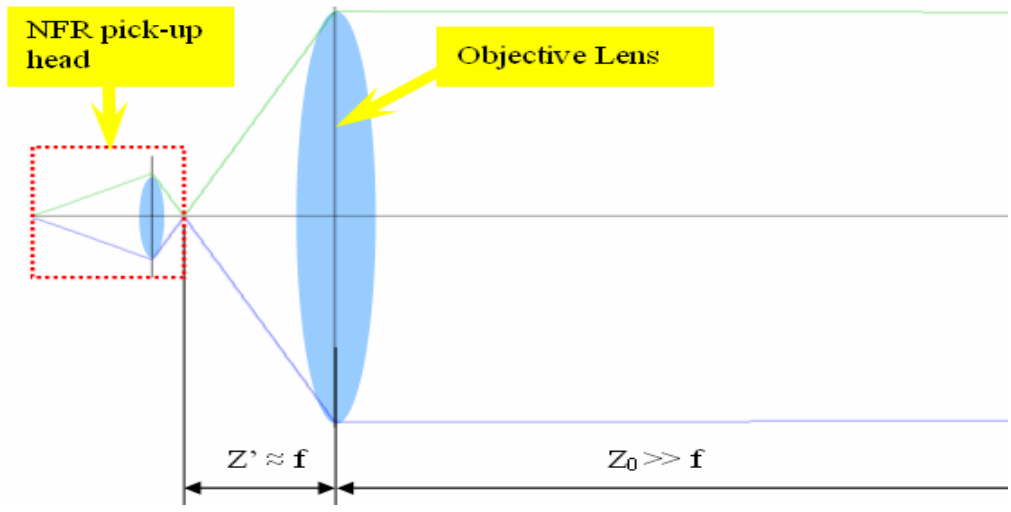

Fig.4-6 A co-focal system in measurement setup

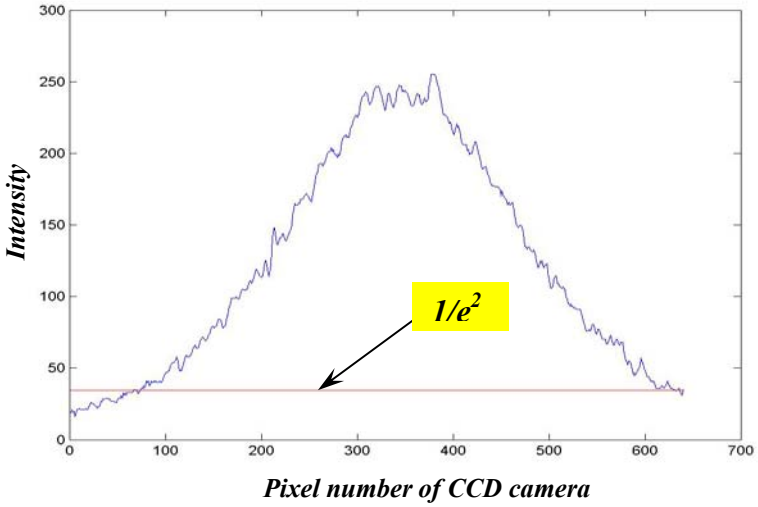

Fig.4-7 Definition of output beam size

This method results in the output beam larger than diffractive limit and will not need precisely control the position of the objective lens and CCD camera. In order to ensure the output beam to be collimated, the spot size is measured and should be remained the same at several positions which are far from the objective lens. What we really measured is the collimated output beam size but not the focused spot size which we want to know, therefore, we use the Gaussian beam condition to calculate spot size according to fundamentals of photonics.

4.2.1 Principle

If a lens is placed at the waist of a Gaussian beam, as shown in Fig.4-8, the transmitted beam is then focused to a waist radius W_0' at a distance z' given by :

$$W_0' = \frac{W_0}{[1+(z_0/f)^2]^{1/2}}$$
$$z' = \frac{f}{1+(f/z_0)^2} \qquad (1)$$

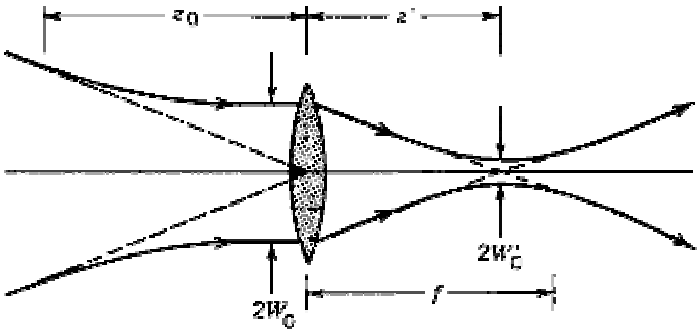

Fig.4-8 Focusing a beam with a lens at the beam waist

If the depth of focus of the incident beam $2z_0$ is much longer than the focal length f of the lens (Fig.4-9), then $W_0' \approx (f/z_0)W_0$. Using $z_0 = \pi W_0^2/\lambda$, we obtain :

$$W_0' = \frac{\lambda}{\pi W_0} f = \theta_0 f$$
$$z' = f \qquad (2)$$

The transmitted beam is then focused at the lens' focal plane as would be expected for parallel rays incident on a lens. This occurs because the incident Gaussian beam is well approximated by a plane wave at its waist. The spot size expected from ray optics is, of course, zero. In wave optics, however, the focused waist radius W_0' is directly proportional to the wavelength and the focal length, and inversely proportional to the radius of the incident beam.

In our condition, it is desirable to generate the smallest possible spot size. It is clear from equation (2) that this may be achieved by use of the shortest possible wavelength, the thickness incident beam, and the shortest focal length. Since the lens should intercept the incident beam, its diameter D must be at least $2W_0$. Assuming that $D = 2W_0$, the diameter of the focused spot is given by :

$$2W_0' \approx \frac{4}{\pi}\lambda F\# \qquad (3)$$
$$F\# = \frac{f}{D}$$

where F# is the F-number of the lens, and D is the pixel of CCD (D=pixel x 7.4 μm). A microscope objective with small F-number is often used. Since equation (2) is approximate, their validity must always be confirmed before use.

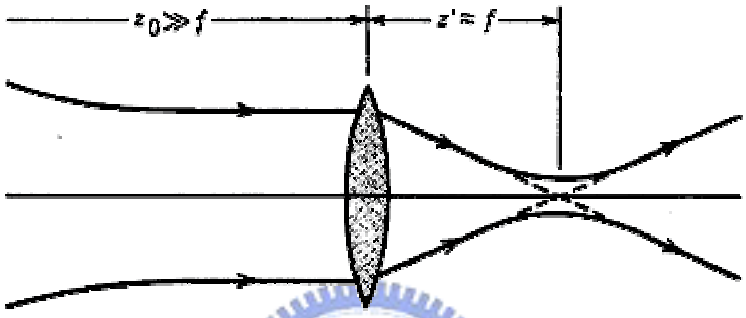

Fig.4-9 Focusing a collimated beam

4.2.2 Experiment Setup

In this research, the far-field measurement system has two different experiment setups, one is for fiberlens measuring setup and the other is for fiberlens with SIL/aperture components measuring setup.

In fiberlens measuring experiment setup, in order to compare with simulation, the spots emitted from the fiberlens were measured and verified. A 633nm laser is coupled into fiber that has a fiberlens in front-end. A 3-axial position stage is used to control the distance between fiberlens and objective lens. A CCD camera is put on the guider, and adjusts the position of the CCD camera from 12cm to 32cm toward objective lens. Compared with the focal length of objective lens is 1.6cm, the distance between objective lens and CCD camera is much larger than the focal length of objective lens. The output beam can be approximated as a collimated beam when the spot size on the

CCD camera remains the same in different positions. Hence the spot size can be calculated by previous principle in 4.2.1 section. The measuring system of fiberlens is shown in Fig.4-10.

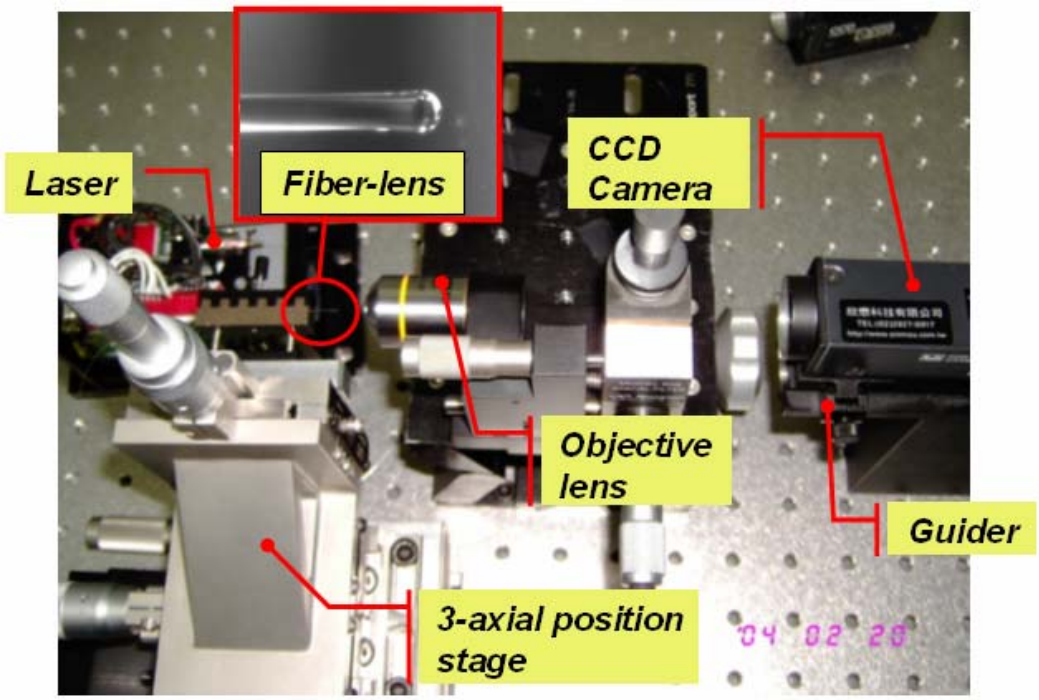

Fig.4-10 Illustration of the fiberlens measuring system

In measuring experiment setup of fiberlens with SIL/aperture components, we used the previous structure to measure the properties of fiberlens. Then adding the other 3-axial position stage for sample adjusting to control the position of sample, and the optical microscope (OM) system is employed to capture the distance between the fiberlens and sample. Adjusting the position of objective lens make the output beam collimated. Changing the position of sample makes it close to the optimum position according to the spot size which capture from CCD camera. Finally, the final output beam was measured by CCD camera system. The measurement system of fiberlens with SIL/aperture component is shown in Fig.4-11.

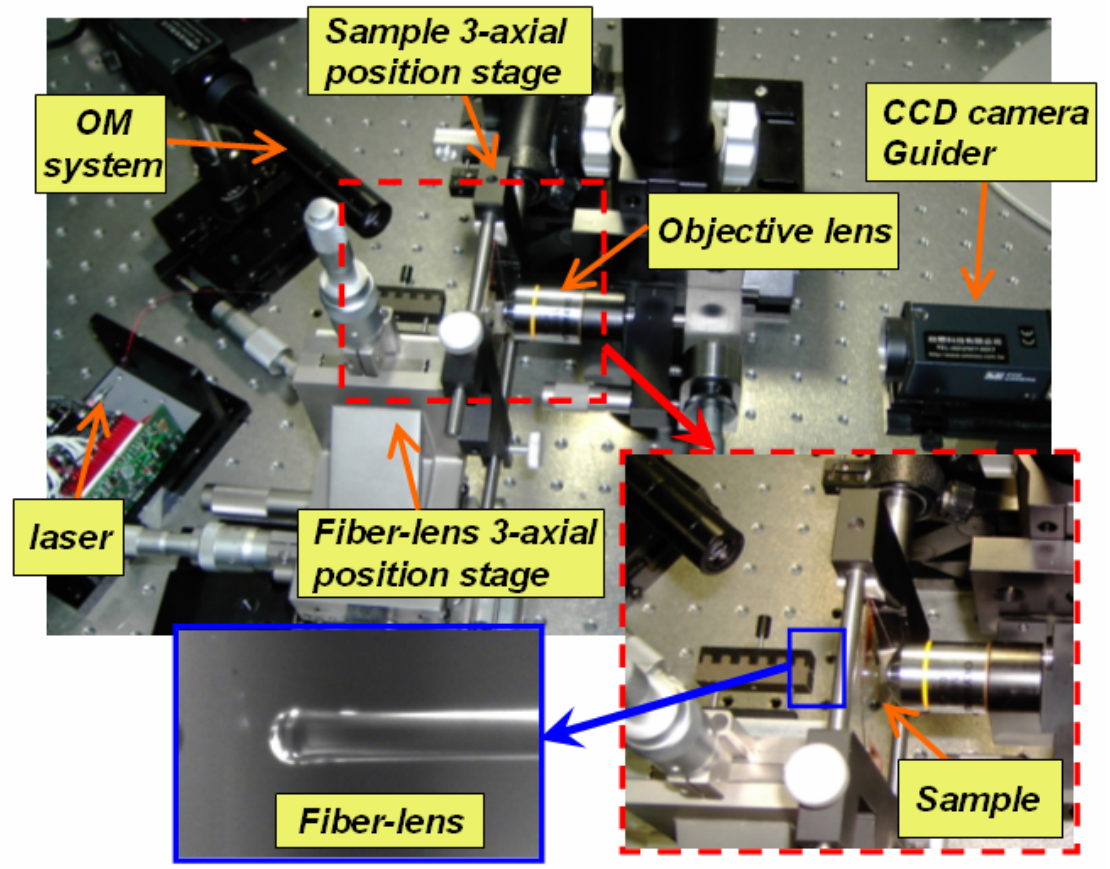

Fig. 4-11 Illustration of the fiberlens with SIL/aperture component measuring system

In this measurement system, the equipments including 3-axial position stage, objective lens, CCD camera, and capture card will be presented. The 3-axial position stages are used to control the position of fiberlens and sample. The resolution of the position stage used is 0.5μm, so we can precisely control the alignment of each component. The specification of CCD camera is listed in Tab.4-4. In order to improve the accuracy, the sensing area of CCD camera is square. The spot diagraph is captured by capture card without compression. Then we wrote the program using Matlab to get the profile of the spot, and to analyze the spot size. Since the ambient light has an influence on our measurement. The intensity of ambient light was measured to be compared with the intensity of spot, and to be used as the background noise to correct the measured data, as shown in Fig.4-12.

Tab.4-4 Specification of CCD camera

Pick-up device	1/3 type CCD
Effective picture elements	659(H) X 497(V)
Sensing area	7.4μm X 7.4μm
Horizontal frequency	15.734 kHz
Vertical frequency	59.94 Hz

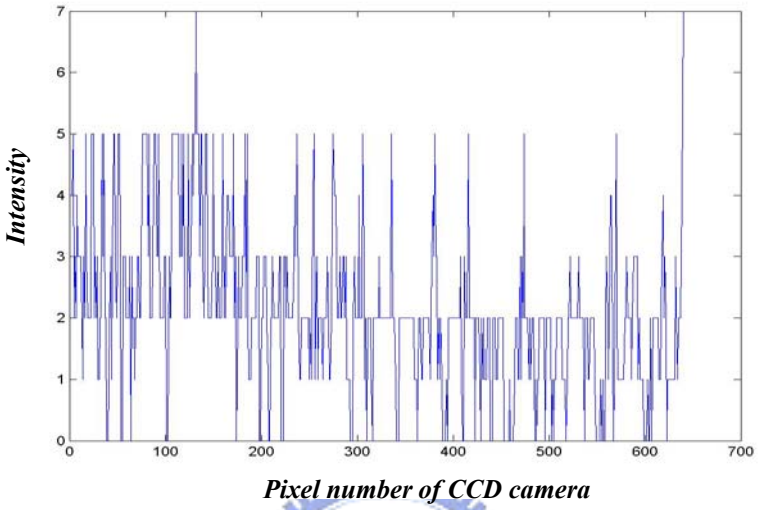

Fig.4-12 Intensity of ambient

4.2.3 Self-Alignment Verification

The self-alignment between the SIL and aperture is verified by measuring experiment setup of fiberlens with SIL/aperture component. Owing to the pattern of aperture and opening ring is a concentric circle structure, and fabricated in the same process step. This opening ring is employed to fabricate the SIL in backside exposure step. Hence the aperture and SIL will be aligned together precisely by self-alignment technique. The measurement result of self-alignment verification is shown in Fig.4-13. From the figure 4-13, we found that the laser passing through the opening ring and SIL with aperture in the bottom of SIL can be observed a concentric circle light source. This result verifies the feasibility of the proposed self-alignment technique.

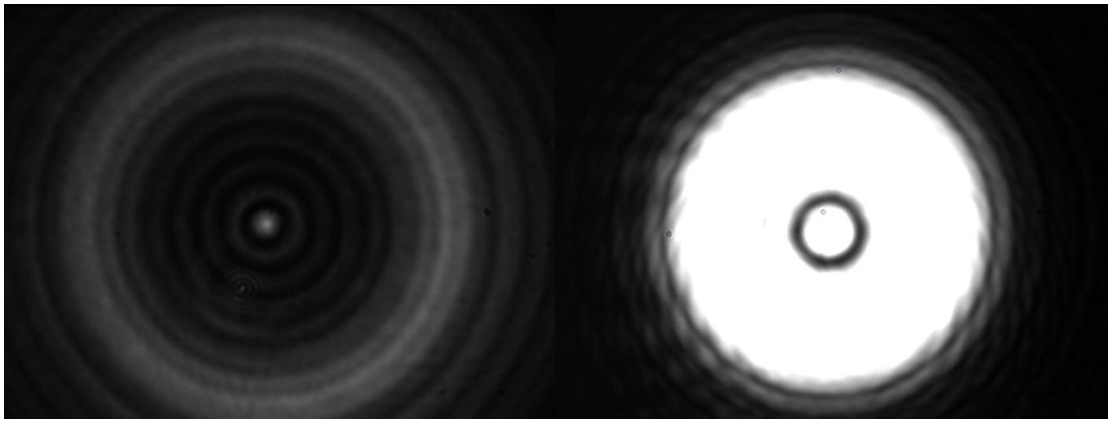

Fig.4-13 The measurement result of self-alignment verification

4.2.4 Spot Size Calibration

In spot size calibration, we aim two measuring result, one is for fiberlens only and the other is for fiberlens with SIL/aperture component.

We fabricated a fiberlens with a length 465 μm which used microscope to measure the length of fiberlens precisely. This fiberlens has a radius 62.5 μm as shown in Fig.4-14, and it will be measured by the previous far-field experiment setup in 4.2.2 section.

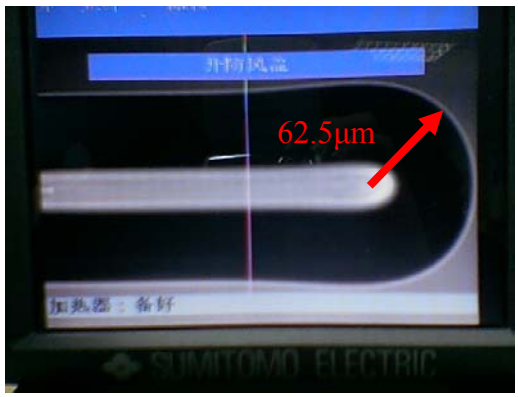

Fig.4-14 Photograph of fiberlens with radius 62.5 μm

The measurement results are captured by CCD camera, and then used the Matlab software to calculate and analysis. The output beam profile can be obtained. Finally, the spot size can be calculated by the formula in 4.2.1 section from output beam profile. The output beam profile measurement result of fiberlens is shown in Fig.4-15, and the spot size 2.99 μm is obtained.

Here, the fiberlens combining the SIL and aperture components is also measured by far-field experiment setup in 4.2.2 section. The SIL component has two different size including the diameter 60 μm and 70 μm. The detail sizes of SIL which is made by fabrication process are listed in Tab.3-5.

First, the fiberlens combines the aperture and SIL component that has 28.56 μm radius and 29.63 μm sag height as shown in Tab.3-5, and the output beam profile is shown in Fig.4-16. The measurement result of spot size in this case is 2.09 μm.

Next, the fiberlens combines the aperture and SIL component that has 33.52 μm radius and 31.44 μm sag height as shown in Tab.3-5, and the output beam profile is shown in Fig.4-17. The measurement result of spot size in this case is 2.12 μm.

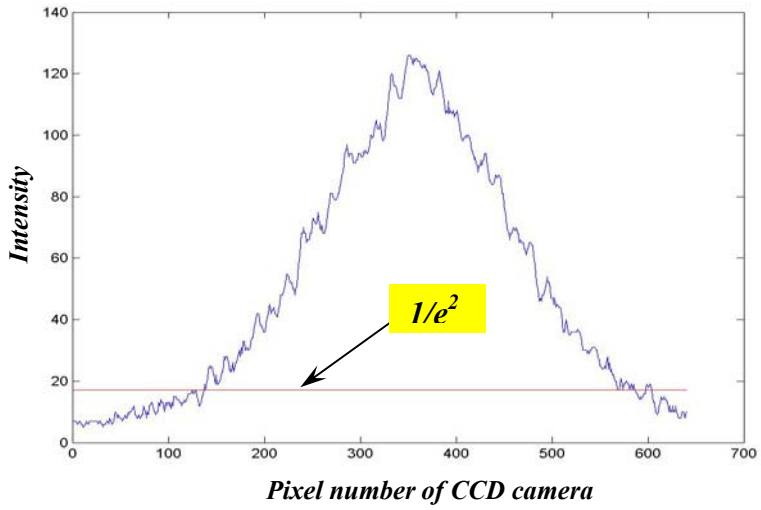

Fig.4-15 The beam profile of fiberlens with 2.99 μm spot size

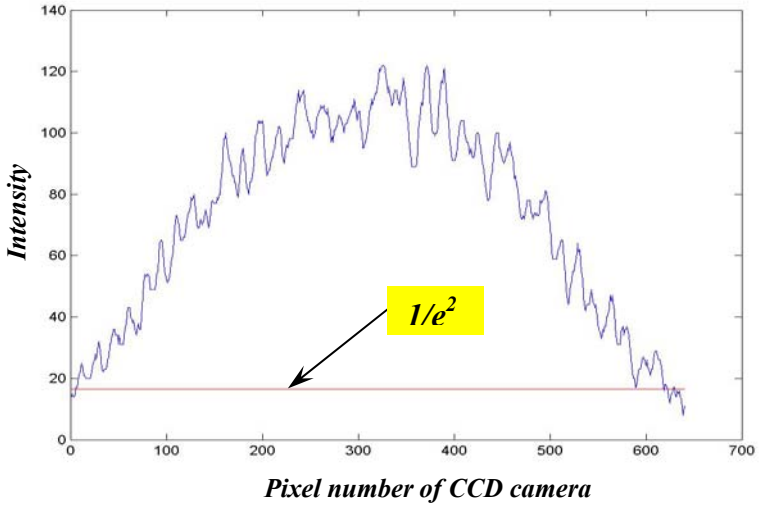

Fig.4-16 The beam profile of fiberlens with aperture/ φ 60 SIL with 2.09 μ m spot size

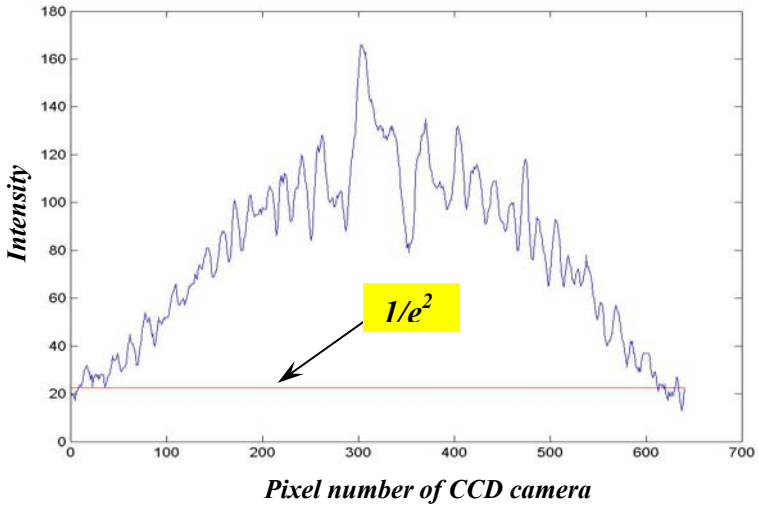

Fig.4-17 The beam profile of fiberlens with aperture/ φ 70 SIL with 2.12 μ m spot size

The simulation and measurement results of spot size are listed in Tab.4-5. We found that the deviation in spot size of fiberlens is less than 0.5%, this results are very perfect in our research. But the deviations in spot size of fiberlens with φ60 SIL and φ70 SIL have 10.05% and 4.25%, respectively, this result are so bad. Because the surface profile of SIL in simulation condition is assumed a perfect hemisphere, but the actual surface profile of SIL in fabrication process result is not a perfect hemisphere. For this reason, it will cause a larger deviation in spot size of fiberlens with SIL

component due to the discordant surface profile of SIL. Furthermore, the measurement results of spot size in fiberlens with φ60 SIL and φ70 SIL component have 30.1% and 29.1% shrinkage efficiency.

Tab.4-5 The simulation and measurement results of spot size

	Diameter (μm)	*Spot size of simulation results (μm)*	*Spot size of measurement results (μm)*	*Deviation (%)*
Fiberlens	**--**	3.00	2.99	0.33
SIL	φ60	1.88	2.09	10.05
	φ70	`2.03	2.12	4.25

4.2.5 SIL Reliability

We measure the reliability of SIL including transmission efficiency, and spot size calibration before and after laser destruction with 6mW/cm^2 light intensity.

The transmission efficiency is measured by Power-Meter. The output beam of fiberlens is measured with light intensity 181nW/cm^2, and then we add the SIL into this fiberlens. The output beam of fiberlens combining SIL component has 89nW/cm^2 light intensity. In transmission efficiency measurement, the sag height of SIL is about 30 μm, and the intensity of ambient is about 0.04nW/cm^2. Owing to the intensity of ambient is less than the measure results of light intensity in sample over 10 times, so this measurement results is believable. From measurement results we can find that the transmission efficiency is about 50%, this results matches the designed parameters.

The spot size calibration before and after laser destruction is also measured by experiment setup in 4.2.2 section. The laser source is used with 6mW/cm^2 light intensity. Before laser destruction, the SIL of diameter 60 μm and 70 μm are measured the spot size with 2.02 μm and 2.08 μm as shown in Fig.4-18(a) and

Fig.4-18(b), respectively. After laser destruction, the SIL of diameter 60 μm and 70 μm are measured the spot size with 2.01 μm and 2.12 μm as shown in Fig.4-19(a) and Fig.4-19(b), respectively. The deviation in this measurement is very small, it may be an error in measuring process, and is caused by experiment setup. This measurement results is very perfect in our research. Because we can prove that the SIL is stable and reliable in pick-up head application. The photograph of SIL after laser destruction is captured by SEM system, as shown Fig.4-20. From this picture we can observe that the SIL has not any change.

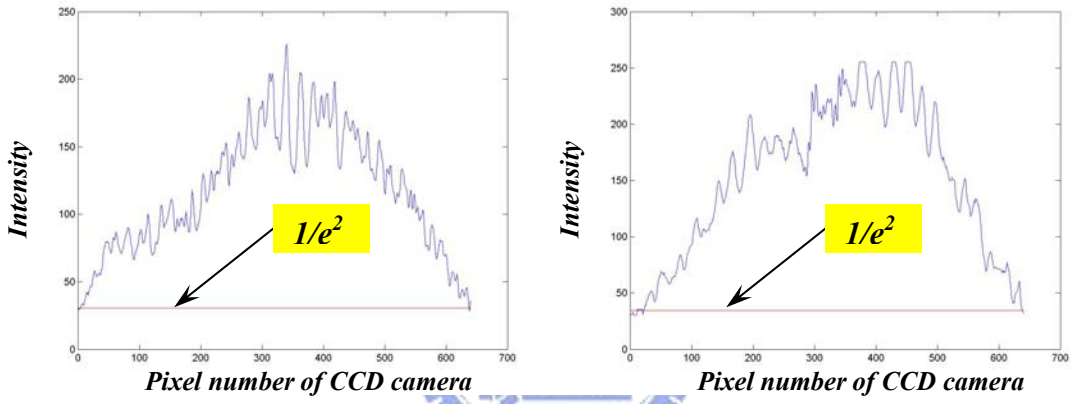

(a) (b)

Fig.4-18 SIL before laser destruction (a) φ60 with 2.02 μm spot size (b) φ70 with 2.08 μm spot size

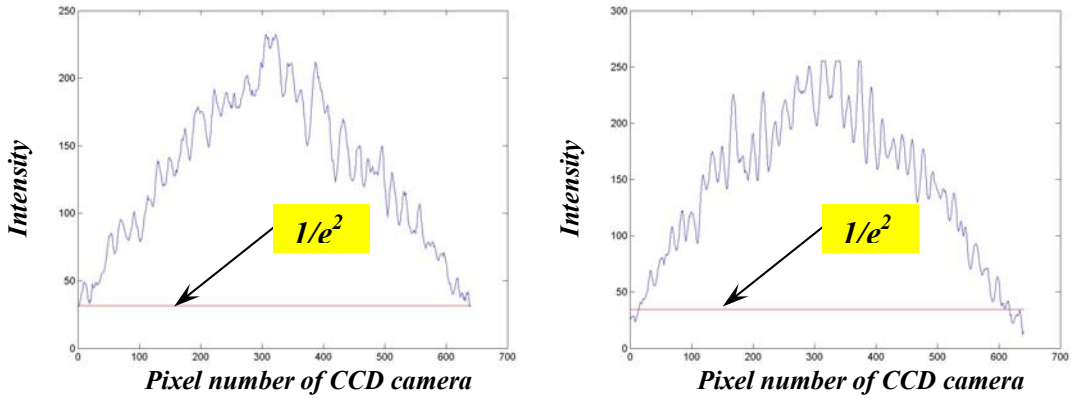

(a) (b)

Fig.4-19 SIL after laser destruction (a) φ60 with 2.01 μm spot size (b) φ70 with 2.12 μm spot size

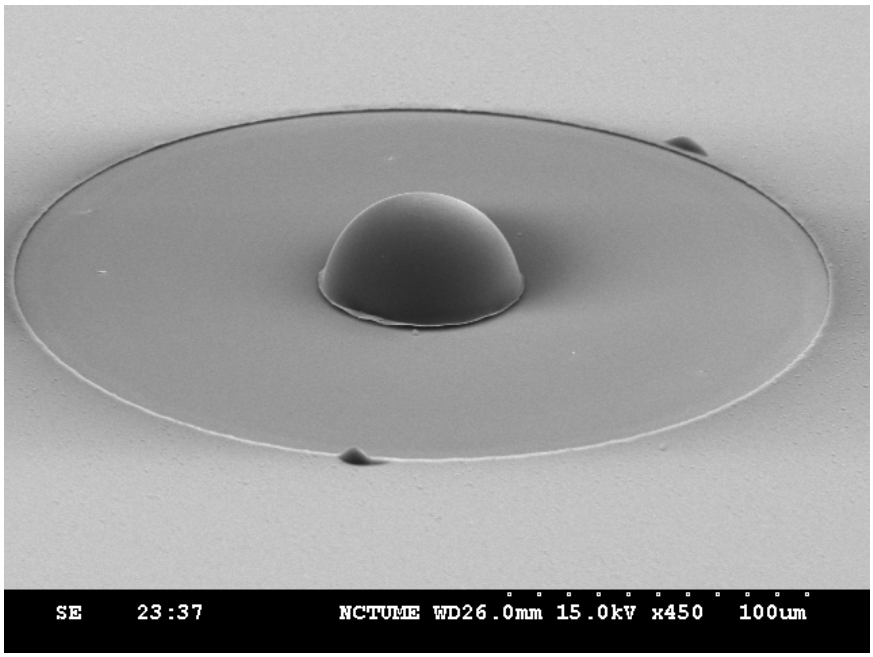

Fig.4-20 The photograph of SIL after laser destruction